ELSEVIER

Polymer 43 (2002) 629–635

polymer

www.elsevier.com/locate/polymer

Comparison of the diffusion coefficients of linear and cyclic alkanes ☆

Rahmi Ozisik[a,*], Ernst D. von Meerwall[a,b], Wayne L. Mattice[a]

[a]*Maurice Morton Institute of Polymer Science, University of Akron, Akron, OH 44325-3909, USA*
[b]*Department of Physics, University of Akron, Akron, OH 44325-4001, USA*

Abstract

Monte Carlo simulations of linear and cyclic alkanes were performed on a coarse-grained high coordination lattice. The simulations were performed at 473 K for C_NH_{2N+2} and C_NH_{2N} where N had the values of 60, 100, and 316. The results indicated: (i) at low molecular weights, cyclic alkanes have lower diffusion coefficients than linear alkanes, and (ii) at high molecular weights, they have higher diffusion coefficients than linear alkanes. The lower diffusion coefficient of the small cyclic alkanes was attributed to the high local density within the volume defined by the smaller mean square radius of gyration of the cyclic alkanes. The high local density of cyclic alkane segments resulted in a decrease in the mobility of the beads. The crossover in diffusion coefficients was observed around the entanglement molecular weight of linear alkanes, which suggests that the linear alkanes are more susceptible to the effects of entanglements than are the cyclic alkanes.

Keywords: Monte Carlo; Diffusion; Alkane

1. Introduction

Cyclic alkanes have been used in crystallization studies, particularly in the determination of the onset of chain folding in linear alkanes [1–3]. The cyclic chains are also important with respect to the reptation theory [4,5] where topological constraints confine a polymer chain in a tube, and movement occurs along the chain contour except at the chain ends [5]. Obviously, a cyclic chain with no chain ends does not fit the simple description of the motion put forth by the reptation theory. It has been argued that the motion of the cyclic chains should be slower than that of linear chains [6,7]. Experiments on networks [8] and solutions [9–11] of linear and cyclic poly(dimethyl siloxane) (PDMS) chains showed higher diffusivity values for cyclic PDMS. And finally, simulations on alkanes have shown that the cyclic alkanes diffuse faster than linear alkanes [12–14]. This work aims to focus on the simulation of alkane chains, but we will compare and discuss the results of the PDMS experiments throughout the paper.

One of the most important works on the cyclic bulk systems was performed by Orrah et al. [15,16]. They measured the bulk viscosities of PDMS chains below and above the critical entanglement molecular weight. Their results showed that: (i) the critical entanglement molecular weight for cyclic PDMS does not differ from the linear PDMS value significantly, (ii) the bulk viscosity of cyclic PDMS is higher than that of linear PDMS at low molecular weights, (iii) the bulk viscosity of cyclic PDMS is lower than that of the linear PDMS at high molecular weights (above the critical entanglement molecular weight), and (iv) the observed crossover in the viscosity is below the entanglement molecular weights of both linear and cyclic PDMS. These results indicate that a similar crossover between the linear and cyclic PDMS chains can be expected for the diffusion coefficients. These results contradict the findings of the spreading boundary technique measurements in solutions [9,10] and network sorption measurements [8] at low molecular weights.

In 1996, Muller et al. [12] performed bulk simulations of cyclic alkanes for degrees of polymerization, N, of 16–512, using the bond fluctuation method (BFM). The size of the cyclic chains was found to be smaller than that of the linear chains at the same degree of polymerization. The root-mean-square radius of gyration ($\langle R_g^2 \rangle^{1/2}$) of the cyclic chains scaled around $N^{0.45}$ ($N^{0.39\pm0.03}$ when extrapolated to infinite molecular weight) compared to $N^{0.5}$ for a linear chain. Muller et al. [12] attributed this lower power law index to Flory-like topological interactions. The dynamics of cyclic alkanes was found to be similar to the dynamics of the linear

☆ This paper was originally submitted to *Computational and Theoretical Polymer Science*. Following the incorporation of *Computational and Theoretical Polymer Science* into *Polymer*, this paper was consequently accepted for publication in *Polymer*.

* Corresponding author. Present address: Institute of Polymers, Swiss Federal Institute of Technology (ETH Zentrum), CNB E98.2, Universitatstrasse 6, CH-8092 Zurich, Switzerland.

E-mail address: ozisik@ifp.mat.ethz.ch (R. Ozisik).

0032-3861/02/$ - see front matter
PII: S0032-3861(01)00417-7

chains, although Muller et al. [12] did not observe any entanglement effects over the molecular weight range that was studied. At low N, the diffusion coefficients of linear and cyclic chains were very similar. At high N, Muller et al. [12] observed a scaling of the diffusion coefficient of the form $N^{-1.2236}$ compared to $N^{-1.5}$ for the linear chains, with cyclic chains having higher diffusion coefficients.

In 1998, Brown and Szamel [13,14], also using BFM, found that the radius of gyration of the cyclic chains scaled around $N^{0.42}$. They also found that the dynamics of cyclic chains was similar to the dynamics of the linear chains. At high N, Brown and Szamel [13,14] observed that the diffusion coefficients of cyclic chains scaled as $N^{-1.54}$, with cyclic chains having higher diffusion coefficients. They argued that the faster dynamics of cyclics originate from their smaller sizes. The smaller sizes of cyclics resulted in a denser (more compact) environment, and therefore the monomers of cyclic chains were shielded from the neighboring molecules more effectively, which resulted in lower interpenetration. This was shown by the larger correlation hole of cyclic chains when compared to linear chains. Brown and Szamel [13,14] concluded that because of this lower interpenetration, the cyclics did not show entanglement in the molecular weight range studied, and therefore diffused faster than linear chains.

At nearly the same time, Doruker and Mattice [17] reported preliminary results for cyclic chains with $N = 100$ and 316 using a different lattice and a different method for coarse-graining the hydrocarbons. The root-mean-square radius of gyration scaled as $N^{0.557}$ for linear chains and $N^{0.486}$ for the cyclic chains. These exponents are larger than those obtained by Muller et al. [12], and Brown and Szamel [13,14]. At $N = 100$, the mean square displacements of linear and cyclic chains overlapped each other. At $N = 316$, the displacements of the cyclic chains were similar to those of the linear chains at short times, but were higher at long times. Doruker and Mattice [17] did not extract the diffusion coefficients from their data, in part because they used short-range interactions but not long-range interactions to decrease the computation time.

This study uses a similar method to that used by Doruker and Mattice [17], but with inclusion of both short- and long-range interactions. The bulk simulations of linear and cyclic alkanes are performed on a high coordination lattice with the use of an on-lattice coarse-graining method and Monte Carlo (MC) algorithm that was first proposed by Rapold and Mattice [18] in 1995. The lattice was named the second nearest neighbor diamond lattice (2nnd). The 2nnd lattice is derived from the diamond lattice by eliminating every other lattice site. The coarse-graining procedure maps two backbone carbon atoms of an ethylene onto one bead [18]. This mapping procedure was shown to be reversible at any time during the simulation [19], which makes the 2nnd a very strong method in the simulation of polymers. With the use of a fast MC algorithm, the 2nnd approach can achieve bulk simulations of polyethylene (PE) faster than a fully atomistic molecular dynamics (MD) simulation depending on the details of the implementation. In the case of $C_{100}H_{202}$, the ratio of MD to MC computer time was found to be around 35 [17]. The conversion of Monte Carlo time step (MCS) to real time step varied between 1 and 171 fs for the $C_{44}H_{90}$ depending on the extent of the long-range interactions and type of parameter set used [17].

2. Simulation setup

Three different pairs of linear and cyclic alkanes with carbon numbers 60, 100, and 316 were used in the simulations. All of the simulations in this study were performed at 473 K, which is higher than the melting temperature, but lower than the boiling temperatures of the alkanes studied [20,21]. The lattice size was $21 \times 22 \times 22$ lattice units for 60 and 100 carbon numbers, and $28 \times 28 \times 28$ lattice units for 316 carbon number. Each lattice unit on the 2nnd lattice corresponds to 2.5 Å, which is determined by the distance between next neighbor carbon atoms (with a bond length of 1.53 Å and a bond angle of 109.5°). The number of chains and corresponding densities of each system are given in Table 1 for the linear and cyclic alkanes.

The densities of the linear alkanes were determined according to the following equation, which was first developed by von Meerwall et al. [22]

$$\rho(M,T) = \left[\frac{1}{\rho(M \to \infty, T)} + 2\frac{V_e(T)}{M} \right]^{-1} \qquad (\mathrm{g/cm^3}) \quad (1)$$

This density equation is the result of a fitting of a collection of densities from the literature with two fitting parameters that are given with the following equations [22]:

$$\frac{1}{\rho(M \to \infty, T)} = 1.142 + 0.00076T\ (^\circ\mathrm{C}) \qquad (\mathrm{cm^3/g}) \quad (2)$$

and

$$V_e(T) = 13.93 + 0.06T\ (^\circ\mathrm{C}) \qquad (\mathrm{cm^3/mol}) \quad (3)$$

The uncertainties in these quantities are 0.005 cm^3/g and 0.3 cm^3/mol, respectively. It is expected that extrapolations

Table 1
The simulation setup for the linear and cyclic alkanes. Target densities were calculated from Eq. (1) at 473 K

System	Number of chains	Occupancy (%)	Target density (g/cm^3)	Simulation density (g/cm^3)
$C_{60}H_{122}$	59	17.41	0.738	0.733
$C_{100}H_{202}$	36	17.71	0.751	0.745
$C_{316}H_{634}$	25	17.99	0.766	0.757
$C_{60}H_{120}$	59	17.41	0.738	0.733
$C_{100}H_{200}$	36	17.71	0.751	0.745
$C_{316}H_{632}$	25	17.99	0.766	0.757

of the density equation to higher molecular weight (M) will not systematically deviate, but their uncertainties will increase substantially [22]. Beevers et al. [23] performed density measurements on PDMS systems and found that: (i) the density of cyclic PDMS is higher than that of linear PDMS at the same molecular weight, (ii) the densities of %linear and cyclic PDMS chains approached each other with increasing molecular weight. If similar behavior is expected from alkanes, then these simulations would overestimate the density of cyclic alkanes, particularly at low molecular weights. Since the densities of cyclic alkanes are not known, the same melt density was used for linear and cyclic alkanes with the same degree of polymerization. Obviously, this approximation has very critical implications, but until the densities of cyclic alkanes are determined by experiments, the approximation is a necessity.

The short-range (R3) and long-range (L2) interaction parameters used in this study were taken from Ref. [17]. The short-range interaction parameter set used the energies $E_\sigma = 2.7$ kJ/mol, $E_\omega = 14.6$ kJ/mol for first- and second-order interactions in the rotational isomeric state model. These energies specify the statistical weights $\sigma = 0.503$ and $\omega = 0.024$ at 473 K. The long-range interaction parameter set used the Lennard–Jones (LJ) parameters $\epsilon/k = 185$ K and $\sigma = 4.4$ Å. These LJ parameters were used to calculate the 2nnd lattice shell energies [24]. This study uses three shells that have the following interaction energies: $u_i = 15.022$, 0.620, and -0.624 kJ/mol, where $i = 1$–3. Double occupancy of any site is prohibited during the simulation (both equilibration and sampling stages).

The simulation proceeds by single-bead moves to neighboring sites, with the acceptance of each proposed move being judged by the Metropolis criteria. All systems were equilibrated in two steps before the simulation. The duration of the first equilibration varied between 10 and 20 million Monte Carlo steps (MCS) depending on the system size. During this initial equilibration step, the long-range interactions were turned off. The duration of the second equilibration was 10 million MCS for all systems, and the second equilibration process was performed with full potentials (short- and long-range interactions turned on). The change in the energy of the system was followed during the equilibration in order to verify that the system became stable. The purpose of the equilibration step is to enable the system to evolve from the starting conformation to reach equilibrium. We used a two-step equilibration in order to achieve faster results. The initial equilibration required less computer time because only short-range interactions were used. The second equilibration step was performed with full potentials, which is much slower than the first equilibration step, but is necessary to eliminate any contacts that have high interaction energies (e.g., first shell long-range interactions). The data were collected at every 500 MCS for a total time of 10 million MCS for carbon numbers 60 and 100, and at every 5000 MCS for a total time of 20 million MCS for carbon number 316.

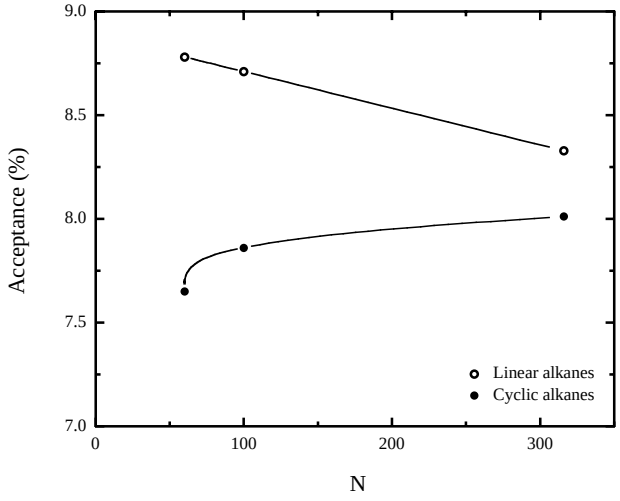

Fig. 1. Acceptance rates of the single bead moves on the 2nnd lattice.

3. Results and discussion

3.1. Acceptance rates and the occupancy of the shells

The acceptance rates for the single-bead moves on the 2nnd lattice are shown in Fig. 1. The acceptance rates of linear and cyclic alkanes showed opposite tendencies, and the difference between the acceptance rates of linear and cyclic alkanes decreased with increasing N. Both acceptance rates should reach the same limit as $N \rightarrow \infty$.

The shell occupancy values for the three shells used in the energy calculations are given in Fig. 2. The occupancy values increase as the shell number increases, as expected

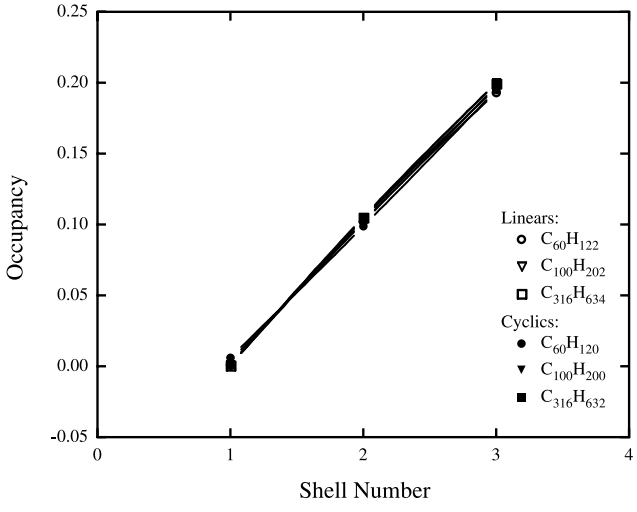

Fig. 2. Occupancy of the neighboring shells on the 2nnd lattice with respect to shell number.

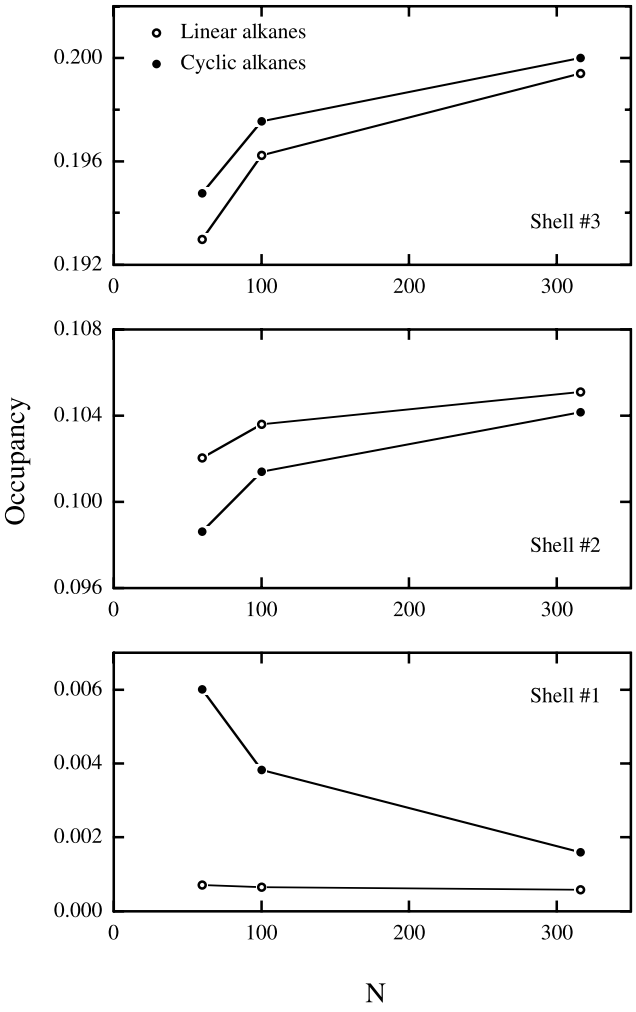

Fig. 3. Occupancy of the neighboring shells on the 2nnd lattice with respect to the number of carbon atoms.

from the sizes of the u_i. A closer look at the occupancy values with respect to N is given in Fig. 3. The (absolute) difference between the occupancy values of linear and cyclic alkanes decreased with increasing N. This, combined with the acceptance rates, suggests that the cyclic alkanes behave more and more like linear alkanes as the molecular weight increases.

At the first neighboring shell, the cyclic alkanes show a much higher occupancy value than the linear alkanes. In

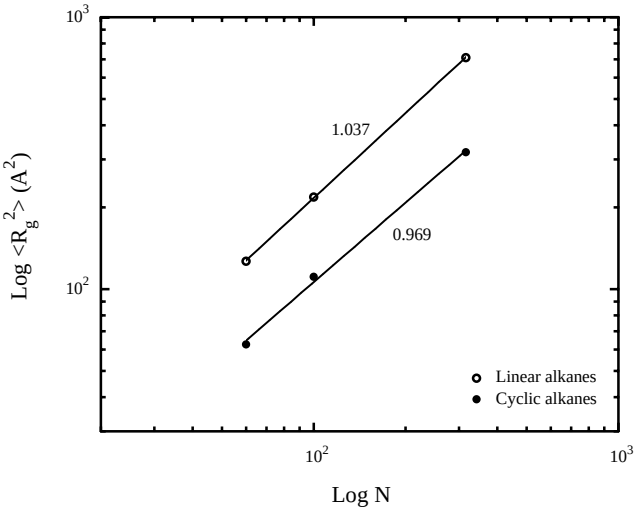

Fig. 4. Mean square radius of gyration of linear and cyclic alkanes from 2nnd lattice simulations.

fact, the occupancy of the cyclic alkanes at the first shell is 8.6, 6.3, and 2.7 times that of the linear alkanes for $N =$ 60, 100, and 316, respectively. These high occupancy values indicate, as expected, that the local density of the cyclic alkanes is larger than that of the linear chains. It should also be noted that the ratio of the occupancy values of the cyclic and linear alkanes decreased with N, and the values should approach a common limit as $N \rightarrow \infty$.

3.2. Static properties

The static properties of the linear and cyclic chain simulations are given in Table 2. The properties are given as 'property $\pm x_p$', where x_p is the standard deviation and is given by the following expression:

$$x_p = (\langle p^{2i} \rangle - \langle p^i \rangle^2)^{1/2} \quad (4)$$

where p is the property, and i is an integer. In Table 2, i takes on values of one for the mean end-to-end distance, $\langle R \rangle$, and two for the mean square end-to-end distance, $\langle R^2 \rangle$, and mean square radius of gyration, $\langle R_g^2 \rangle$.

The sizes of the linear and cyclic alkanes were compared in terms of $\langle R_g^2 \rangle$ (see Fig. 4). The linear alkanes are almost twice the size of the cyclic chains, as expected for long random flight chains. The root-mean-square radius of

Table 2
The static properties of the linear and cyclic alkanes, and the corresponding standard deviations. See Eq. (4) for the definition of ' ± ' in the table

System	$\langle R_g^2 \rangle$ (Å^2)	$\langle R^2 \rangle$ (Å^2)	$\langle R \rangle$ (Å)	$\langle R^2 \rangle / \langle R_g^2 \rangle$	$\langle R^4 \rangle / \langle R^2 \rangle^2$	C
$C_{60}H_{122}$	126.5 ± 50.2	846 ± 570	27.30 ± 10.01	6.69	1.45	6.23
$C_{100}H_{202}$	218.4 ± 95.6	1362 ± 989	34.45 ± 13.21	6.24	1.53	5.94
$C_{316}H_{634}$	711.0 ± 358.8	4335 ± 3370	60.90 ± 25.03	6.10	1.60	5.90
$C_{60}H_{120}$	62.67 ± 14.01					
$C_{100}H_{200}$	110.9 ± 31.41					
$C_{316}H_{632}$	319.2 ± 89.12					

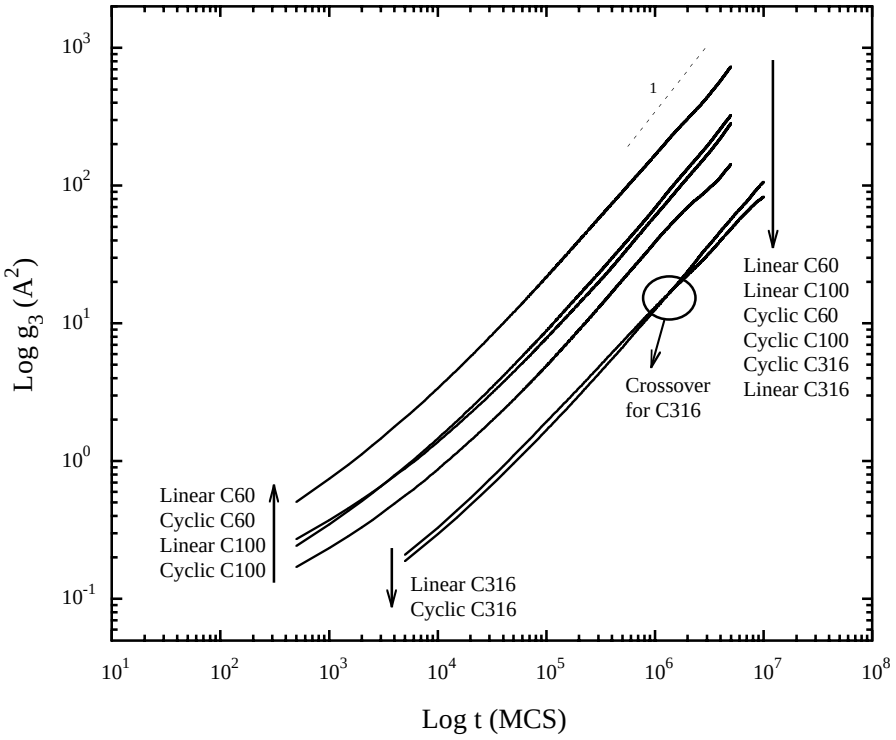

Fig. 5. Mean square center of mass displacement of linear and cyclic chains.

gyration scaled with $N^{0.52}$ for linear chains and $N^{0.48}$ for cyclic chains. The error in the power law index values (arising from the standard deviation of $\langle R_g^2 \rangle$) is around 0.03 and 0.02 for linear and cyclic chains, respectively.

The power law index of 0.52 for the linear alkanes is larger than the estimate 0.4 that was given by Cates and Deutsch [25], and is comparable with the value of 0.553 that was given by Brereton and Vilgis [26]. Also, the dimensionless ratio $\langle R^4 \rangle / \langle R^2 \rangle^2$ approached the Gaussian limit of 5/3, and the dimensionless ratio of $\langle R^2 \rangle / \langle R_g^2 \rangle$ approached six with increasing N for the linear chains.

3.3. Dynamic properties

3.3.1. Center of mass displacement

The mean square displacement of the center of mass (g_3) for all linear and cyclic chains is given in Fig. 5. The slope of g_3 for all systems increased to 1.0 at long times. This Fickian behavior is expected at long times. The difference between the displacement values of linear and cyclic alkanes at the same N decreases as N increases. This behavior agrees with the N dependency of the differences in the acceptance and occupancy values between linear and cyclic alkanes. There are two crossovers in Fig. 5: (i) the displacements of the cyclic $C_{60}H_{120}$ and linear $C_{100}H_{202}$ crossed each other, where $C_{60}H_{120}$ slowed down compared to $C_{100}H_{202}$, and (ii) the displacements of the cyclic and linear alkanes for $N = 316$. Obviously, the important crossover is the second one because it reflects a change in the behaviors of linear and cyclic alkanes at the same N. At $N = 316$, the initial displacement values of linear and cyclic alkanes are similar both in starting value and slope, and they remain close throughout the simulation. The crossover is observed at long times, where the slope values approach unity.

3.3.2. Diffusion coefficients

The long time Einstein diffusion coefficients of all systems are shown in Fig. 6 with respect to N, and in Fig. 7 with respect to the radius of gyration. The straight-line fit of the logarithmic diffusion coefficients of the linear

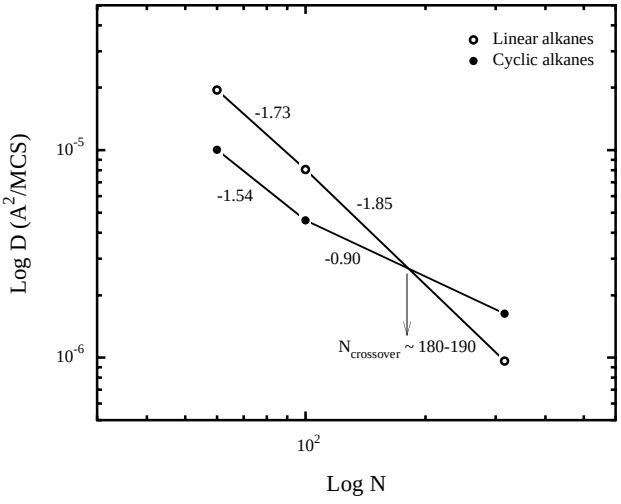

Fig. 6. Diffusion coefficients of linear and cyclic alkanes with respect to the number of carbon atoms.

chains vs. N (Fig. 6) gave an overall slope of -1.82, although the slope changed from -1.73 to -1.85 with increasing N. The slope of -1.73 of the linear chains (at low N) is almost equal to the -1.74 value obtained from the direct pulsed-gradient spin-echo NMR diffusion coefficient measurements of $C_{12}H_{26}$ and $C_{60}H_{122}$ at 473 K [27,28]. This match of the slopes between the experiments and the simulations suggests that the parameter set R3L2 successfully describes the dynamics of the *n*-alkanes. The slope of the diffusion coefficients of the cyclic chains was calculated to be -1.54 at low N and -0.90 at high N. The value of -1.54 at low N is similar to the observations of Brown and Szamel [13,14], although in our case, the cyclic alkanes have lower D values than the linear alkanes.

The crossover between the linear and cyclic diffusion coefficient (D) is clearly seen in Fig. 6. The crossover ($N_{\text{crossover}}$) is around 180–190. This is similar to the crossover observed in the case of PDMS systems [15]. The observed crossover in D cannot be explained with the changes in acceptance and occupancy values alone. The fact that the acceptance and occupancy values of cyclic alkanes approach to those of linear chains with increasing N, results in cyclic alkanes behaving more and more like linear alkanes. And both, the acceptance and occupancy values are essentially a response of the beads to the changing size of the chain (dilution of the strong end effects in a smaller linear alkane, and reduction of the strong topological constrains in a small cyclic alkane). As seen from Fig. 4, there is no crossover in the radius of gyration, and therefore the behavior of the radius of gyration does not cause the crossover observed in D (see Fig. 7). Therefore, other factors are also influencing the observed crossover in D.

The lower D of the cyclic chains at low N can be explained by a combination of factors, mainly by the smaller size of the cyclic chains (although not in the same manner as discussed by Brown and Szamel [13,14]) and the local density produced by segments from the same molecule. Because of the smaller size of the cyclic alkanes, the density of these segments inside the volume occupied by a cyclic alkane (and therefore the 'local' density) is higher than that of a linear chain. This effect is apparent in the occupancy of the neighboring shells. The occupancy of the first shell for the cyclic alkanes is around three to nine times larger (depending on the N) than that of the linear alkanes as shown in Fig. 3. The topological constraints decrease the acceptance ratio of the bead moves in the small cyclic, as given in Fig. 2.

The higher D of the cyclic chains at high N may be due to the different manner in which entanglements affect linear and cyclic chains when N is slightly higher than the entanglement length, $N_{\text{e,linear}}$, for the linear chain. This length is about 60 for polyethylene at 413 K [29]. The linear chains are slowed down by the existence of entanglements, which reflects itself as the smaller power law index of -1.85 (for linear alkanes) at high N. But contrary to linear alkanes, cyclic alkanes do not experience entanglements at this N due to their smaller size, which isolates them from other neighboring chains [12–14].

Our study suggests that even though the dynamics of linear and cyclic alkanes are similar, there are certain factors that separate them from each other. One of these factors, a local factor, influences the interactions of the individual beads (e.g. the high occupancy of the shells and strong topological constraint in the small cyclic alkanes). The second factor, a global factor, influences the interactions of the individual chains (e.g. entanglement effects). It is possible to conclude that the local factors are stronger than the global factors at low molecular weights, where the entanglement effects do not exist for cyclic chains. At low molecular weights the local dynamics, such as the mobility of the beads, are restricted due to the higher occupancy of the first shell, and as a result the dynamics of the system is dominated by the local interactions.

At high molecular weights, the size of the chain may become more important as the entanglements dominate the dynamics of the linear chains. The small size of the cyclic chains might result in less interpenetration between chains, and therefore shields them from forming entanglements at the molecular weight where the linear chains do. As a result, the dynamics of the cyclic chains remain unaffected, whereas the linear chains suffer from the entanglement effects.

The observed crossover between linear and cyclic chains is slightly above the entanglement molecular weight, $N_{\text{e,linear}}$, of linear chains. The position of the crossover with respect to the $N_{\text{e,linear}}$ is different for the PDMS systems [15]. This deviation might be a result of the density approximation that is used for the simulations. If the density of the cyclic system is higher, which it should be, then the cyclic curve in Fig. 6 would shift upwards and the position of the cyclic would move towards low N. Of course, it should also be noted that all simulations performed so far, including this work, failed to capture the existence of entanglements in the

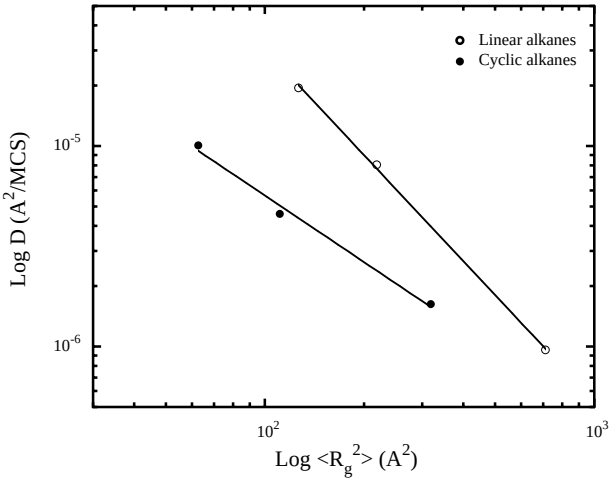

Fig. 7. Diffusion coefficients of linear and cyclic alkanes with respect to radius of gyration.

cyclic chains, whereas the effects of entanglements on cyclic PDMS can clearly be seen from the work of Orrah et al. [15].

4. Conclusions

The cyclic chains showed smaller diffusion coefficients than linear chains below the linear chain entanglement limit of $N_{e,linear} \sim 100$. This observation at low molecular weights does not hold at high molecular weights, where only the linear chains suffer from entanglement effects. At high molecular weights ($N > N_{e,linear}$), cyclic chains are isolated due to their smaller size, and therefore they show higher diffusion coefficients than linear chains. The cross-over in diffusion coefficients of linear and cyclic alkanes was observed at $N \sim 180$–190.

Acknowledgements

This work was supported by National Science Foundation grant DMR 9844069.

References

[1] Lee KS, Wegner G. Linear and cyclic alkanes (C_nH_{2n+2}, C_nH_{2n}) with $n > 100$. Synthesis and evidence for chain folding. Makromol Chem, Rapid Commun 1985;6:203.
[2] Möller M, Cantow H-J, Emeis D, Drotloff H, Lee KS, Wegner G. Phase transitions and defect structures in the lamellar surface of polyethylene and *n*-alkane crystallites. Magic angle spinning carbon-13 NMR studies. Makromol Chem 1986;187:1237.
[3] Percec V, Pugh C, Nuyken O, Pask SD. In: Eastmond GC, Ledwith A, Russo S, Sigwalt P, editors. Comprehensive polymer science, vol. 6. New York: Pergamon Press, 1989.
[4] Doi M, Edwards S. Theory of polymer dynamics. Oxford: Clarendon Press, 1986.
[5] de Gennes PG. Scaling concepts in polymer physics. Ithaca: Cornell University Press, 1979.
[6] Lodge TP, Rotstein NA, Prager S. Dynamics of entangled polymer liquids: do linear chains reptate? Adv Chem Phys 1990;79:1.
[7] Klein J. Dynamics of entangled linear, branched, and cyclic polymers. Macromolecules 1986;19:105.
[8] Garrido L, Mark JL, Clarson SJ, Semlyen JA. Studies of cyclic and linear poly(dimethyl siloxanes): 15. Diffusion coefficients from network sorption measurements. Polym Commun 1984;25:218.
[9] Edwards CJC, Stepto RFT, Semlyen JA. Studies of cyclic and linear poly(dimethyl siloxanes): 5. Diffusion behaviour in dilute solution. Polymer 1980;21:781.
[10] Edwards CJC, Stepto RFT, Semlyen JA. Studies of cyclic and linear poly(dimethyl siloxanes): 7. Diffusion behaviour in a poor solvent. Polymer 1982;23:865.
[11] Higgins JS, Ma K, Nicholson LK, Hayter JB, Dodgson K, Semlyen JA. Studies of cyclic and linear poly(dimethyl siloxanes): 12. Observation of diffusion behaviour by quasielastic neutron scattering. Polymer 1983;24:793.
[12] Muller M, Wittmer JP, Cates ME. Topological effects in ring polymers: a computer simulation study. Phys Rev E 1996;53:5063.
[13] Brown S, Szamel G. Structure and dynamics of ring polymers. J Chem Phys 1998;108:4705.
[14] Brown S, Szamel G. Computer simulation study of the structure and dynamics of ring polymers. J Chem Phys 1998;109:6184.
[15] Orrah DJ, Semlyen JA, Ross-Murphy SB. Studies of cyclic and linear poly(dimethylsiloxanes): 27. Bulk viscosities above the critical molar mass for entanglement. Polymer 1988;29:1452.
[16] Orrah DJ, Semlyen JA, Ross-Murphy SB. Studies of cyclic and linear poly(dimethylsiloxanes): 28. Viscosities and densities of ring and chain poly(dimethylsiloxane) blends. Polymer 1988;29:1455.
[17] Doruker P, Mattice WL. Dynamics of bulk polyethylene on a high coordination lattice. Macromol Symp 1998;133:47.
[18] Rapold RF, Mattice ML. New high-coordination lattice model for rotational isomeric state polymer chains. J Chem Soc, Faraday Trans 1995;16:2435.
[19] Doruker P, Mattice WL. Reverse mapping of coarse-grained polyethylene chains from the second nearest neighbor diamond lattice to an atomistic model in continuous space. Macromolecules 1997;30:5520.
[20] Brandrup J, Immergut EH. Polymer handbook. 2nd ed. New York: Wiley, 1975.
[21] Hocker H. In: Semlyen JA, editor. Cyclic polymers, London: Elsevier, 1986. p. 205–6.
[22] von Meerwall E, Beckman S, Jang J, Mattice WL. Diffusion of *n*-alkanes: free volume and density effects. J Chem Phys 1988;108:4299.
[23] Beevers MS, Mumby SJ, Clarson SJ, Semlyen JA. Studies of cyclic and linear poly(dimethyl siloxanes): 13. Static dielectric measurements and dipole moments. Polymer 1983;24:1565.
[24] Cho J, Mattice WL. Estimation of long-range interaction in coarse-grained rotational isomeric state polyethylene chains on a high coordination lattice. Macromolecules 1997;30:637.
[25] Cates ME, Deutsch JM. Conjectures on the statistics of ring polymers. J Phys (Paris) 1986;47:2121.
[26] Brereton MG, Vilgis TA. The statistical mechanics of a melt of polymer rings. J Phys A 1995;28:1149.
[27] von Meerwall E, Feick EJ, Ozisik R, Mattice WL. Diffusion in binary liquid *n*-alkane and alkane–polyethylene blends. J Chem Phys 1999;111:750.
[28] Ozisik R. Simulation of the dynamic properties of polyethylene melts on the second nearest neighbor diamond lattice. PhD Dissertation, University of Akron, December 1999.
[29] Fetter LJ, Lohse DJ, Colby RH. In: Mark JE, editor. Physical properties of polymers handbook, 2nd ed. New York: American Institute of Physics, 1996. p. 335.